Engineering and Technology Journal
Journal homepage: https://etj.uotechnology.edu.iq

Thermal Behavior Simulation of An Externally Cooled Electric Motor

N. Meneceur [a*], S. Boulahrouz [b], A. Boukhari [a] , R. Meneceur [a]

[a] Mechanical Engineering Dept., Faculty of Technology, University of EL-Oued, 39000 EL-Oued, ALgeria.
[b] Mechanical Engineering Dept., KHENCHELA University, ALGERIA.
*Corresponding author Email: Meneceur-noureddine@univ-eloued.dz

HIGHLIGHTS

- A mathematical model is developed to determine the internal thermal sources .
- A computer program is developed to numerically simulate the proposed model.
- The mitigation of thermal losses is strictly related to the specific speed.

ARTICLE INFO

Handling editor: Muhsin J. Jweeg

Keywords: External cooling, electric motor, fan, transient regime, nodal method.

ABSTRACT

This paper presents the simulation results of the thermal behavior for an externally cooled asynchronous electric motor in both steady and transient states cases. For this purpose, a mathematical model based on the heat equation is first developed to determine internal thermal sources such as copper, mechanical, and iron losses. Then, a computer program is developed to numerically simulate the proposed mathematical model. This program determines the radial distribution of steady and transient states temperatures and predicts the effect of the ambient temperature on the transient and permanent temperature distributions. This makes it possible to calculate the specific speed of the motor as a function of its rotation speed, the airflow rate, and the pressure dropping at the fan level. The obtained results show that the engine heating is mainly due to the elements that show thermal losses by the Joule effect. Moreover, the mitigation of these losses is strictly related to the specific speed, making it possible to select the right choice for the engine cooling system.

1. Introduction

The electric motor dissipation system is thermally non-homogeneous with complex geometry, despite the existence of symmetries. In addition, one of the difficulties encountered in its development is thermal dimensioning. The main problem is that the study of the thermal aspect was lagging behind other electrical, magnetic, and mechanical considerations. The thermal analysis of an engine involves simultaneously the knowledge of power losses transformed into heat and the efficiency of their evacuation (heat losses). In particular, the evaluation problems of the distribution loss, the choice of the flows type, the heat exchanges, the geometric complexity, and the diversity of thermo-physical properties of constituents are mainly considered as troubles sources.

The heating of electric motors causes thermal stresses that particularly affect the life of vital elements such as rolling bearings of the mechanical axis or winding insulators through the appearance of hot spots. Therefore, it is necessary to preserve their time of use and their cost to ensure their protection in operation.

On the other hand, the electric motor has shown the problem of increased thermal usage due to its massive volume and high speed. The increase of the cooling system efficiency for fan motors directly influences enhancing motor reliability and lifetime [1]. Accordingly, many numerical and experimental studies on power loss generation and thermal behavior for large power machines have been developed [2, 3]. One of the most common thermal analysis techniques is the thermal network [4]. In particular, many numerical simulation methods have been proposed for the thermal analysis of the electric motors, especially the finite element method, which is frequently used to estimate the temperature distribution using only the heat conduction [5]. It is worth noting that some researchers on this subject have also been conducted based on the nodal resolution methods, which partially limits the structure of the studied system. Satiraman et al.[6] have proposed a powerful resolution software using the finite element method to resolve complicated geometrical models requiring many computation nodes. Popescu et al.[7] presented a review paper concerning cooling technologies and heat analysis of brushless permanent magnet machines. However, most of the proposed techniques published to date highlighted several thermal design issues that are

http://doi.org/10.30684/etj.2021.131114.1006
Received 11 August 2021; Accepted 21 December 2021; Available online 12 May 2022
2412-0758/University of Technology-Iraq, Baghdad, Iraq

difficult to analyze. Thermal analysis of an electric motor solving the more difficult aspects was conducted by Staton et al.[8]. Sreehivasan and Sengupta [9] used a one-dimensional model to predict electric motors' cooling performance. The authors have determined the heat transfer coefficients on the surface and within the machine. Nevertheless, the internal heat transfer coefficients seem to be unrealistic. Otherwise, an analytical study that predicted both rotor and stator winding temperatures was presented by Dokopoulos and Xypteras [10]. However, they supposed that the model is made of rings placed over each other at constant lengths. An analytical study of the thermal behavior of electric motors was conducted by Staton et al.[11]. This study is an important part of the electric motor design process since it diminishes weights and costs and increases efficiency.

Recently, many researchers have focused on the three-dimensional thermal analysis of a permanent magnet motor with cooling fans. Tan et al. carried out a computational fluid dynamics (CFD) simulation with a thermal consideration.[12]. The authors proposed a simplified numerical approach to study an axial flux permanent magnet machine with a complex configuration in three-dimensional space. The conduction of forced convection and conjugate heat transfer is taken as a case study. Kyuho et al.[13] used a thermal analysis model of a high-speed permanent magnet motor with cooling flows supported on gas foil bearings. The authors investigated the thermal effects of the carrier harmonics, cooling flows, and rotor speed on motor temperature for an effective thermal design for high-speed machines. Melka et al.[14] proposed three ways of heat dissipation improvement from the electric motor windings. They measured during experiments the average winding temperatures at the nominal rate. The first variant of the heat dissipation improvement was based on covering the external surfaces of the machine with high emissivity material that allowed decreasing the temperature of the windings by approximately 4 K. The second variant was based on the application of two types radiators on the external motor surfaces. A novel kind of machine, called a hot air engine, has been developed by Kramer et al. [15] at the Institute of Energy and Chemical Machinery, University of Miskolc. A mathematical model of this new engine was prepared and compared to the real model of the engine. This model has been designed for low-temperature working media. Asynchronous electric motors are generally cooled by air. Fans are the most commonly used cooling devices for heat flow evacuation. Since the asynchronous motor is the site of heat dissipation, the development of numerical simulation tools requires locating heat sources and the modes of internal transfer in the engine. The analytical methods used for numerical simulation are nodal and finite element methods.

Most recently, Nonneman et al. [16] have conducted a thermal analysis of an interior permanent magnet machine using a lumped parameter model. They evaluated several rotor cooling techniques for electric-vehicle-based applications aiming to achieve higher power densities. They revealed that when the rotor of an electric motor contains a hub, shaft-cooling methods are ineffective. In addition, those results were issued from the temperature distributions of the electrical machine resulting from water jacket cooling in combination with the different rotor cooling techniques. However, the most effective cooling approach to minimize permanent magnet temperatures resulted from rotor jet cooling.

An experimental and numerical investigation of a novel heat pipe-based cooling strategy for permanent magnet synchronous motors (PMSMs) was proposed by Yalong et al. [17]. Those researchers have employed heat pipes with potting silicon gelatin (PSG) as a novel thermal management solution to the heat dissipation problem at the end windings of the PMSMs. They used a 3-dimensional heat pipe by introducing them into the gap between the winding and the casing, whereas potting silicon gelatin is used to fix the heat pipes while increasing the contact area. It was found that the obtained results show that this novel approach maintains the lowest temperatures with a maximum decrease of 22.9°C compared to the original motor. Nevertheless, there is only a 10°C decrease for the motor only with heat pipes.

Moreover, the stable running time of the PMSM with this novel cooling technique has increased by about 50.6 s under the peak-load condition, while its counterpart has almost no improvement (i.e., only with heat pipes). Additionally, they established a numerical model. They showed that it could agree well with the experimental data, leading to the possibility of optimizing the proposed heat pipe-based thermal management solution.

A bibliographic review of research works on electric motors performance, and heat and temperature losses are appraised by Gundabattini et al.[18]. They clustered several factors affecting the efficiency, e.g., airgap eccentricity, electromagnetic performance, effect of temperature, and losses. Similarly, they listed several methods of computer-aided analyses by showing the temperature distribution in an induction motor through simulation results with different cooling methods and suggested future research directions, including cryogenic techniques, heat pipes, and phase change materials technology.

Considering the previous discussion, the main objective of this study is to numerically simulate the heat exchanges within an externally cooled asynchronous electric motor. The nodal numerical method was used to determine the radial temperature distribution in both steady and transient states cases under the effect of the ambient temperature. Because the engine heating is mainly due to those elements showing thermal losses by the Joule effect, the obtained results are analyzed and discussed to demonstrate the mitigation of those losses, which are strictly related to the specific speed. This makes it possible to select the right choice of engine cooling system.

More or less brutal load fluctuations can create heating essentially harmful to the sensitive parts of rotating electrical machines during operation. With the appearance of new power supplies and the increase in specific power, it is necessary to predict the thermal behavior of these machines, either through experimental phases or even through the development of a thermal simulation tool. Such an approach could assist in quantifying, separating, and locating the different internal heat sources that generate overheating.

Consequently, in the present study, we are interested in applying the steps of a numerical simulation method to initially predict the permanent and transient distributions of the temperature field within each element of the considered electrical machine. Then, a good choice of the engine cooling system passes by an approach consisting of calculating the engine's specific speed according to its rotational speed, the air volume flux, and the pressure drops at the level of the cooling fan.

The rest of the paper is organized as follows; in section 2, the problem formulation has been done, its physical and mathematical descriptions, the adopted thermal model, and the external cooling fan choice. Furthermore, section three details the numerical resolution of the studied problem thermal behavior. The obtained results have been presented and discussed profoundly in section 4. Finally, some conclusions have been presented.

2. Problem Formulation

2.1 Physical and mathematical descriptions

The engine is the site of several electromagnetic, mechanical, and Joule losses. The knowledge of these losses translated into heat sources can lead well the study of the thermal behavior. Figure 1 illustrates the asynchronous motor losses separation flowchart.

During the functionality of an electric motor, the heat released is distributed throughout the engine and varies with the operating conditions. The heat losses of the motor are distributed over several principal elements within the motor, including winding copper loss, iron core loss, permanent magnet eddy loss, mechanical loss, and stray loss [19].

In this work, the asynchronous electric motor has been studied in a low power-based regime (4 kW) where the rotor is a spiral type with an external fan ensuring the cooling of 375 W not linked to the motor shaft. An axial view of this engine is shown in figure 2. Given the radial and axial symmetries, the study area is considerably reduced. Figures 3 and 4 show the axial and radial demi-cutting of the engine.

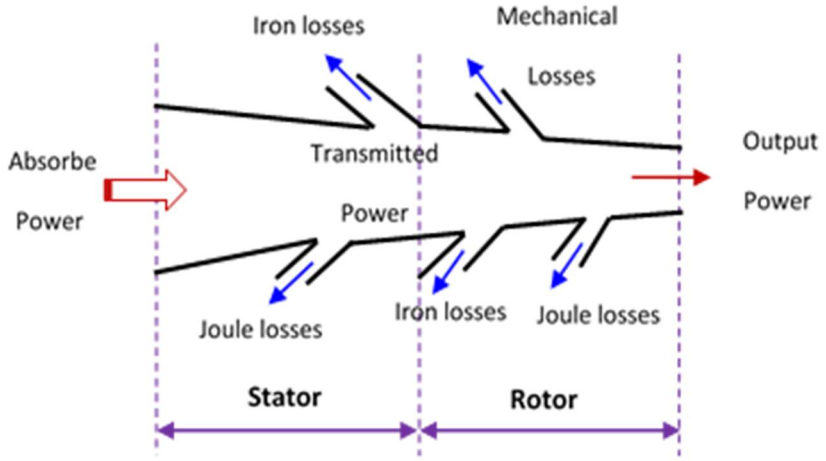

Figure 1: Flow diagram of the heat losses in the electric motor.

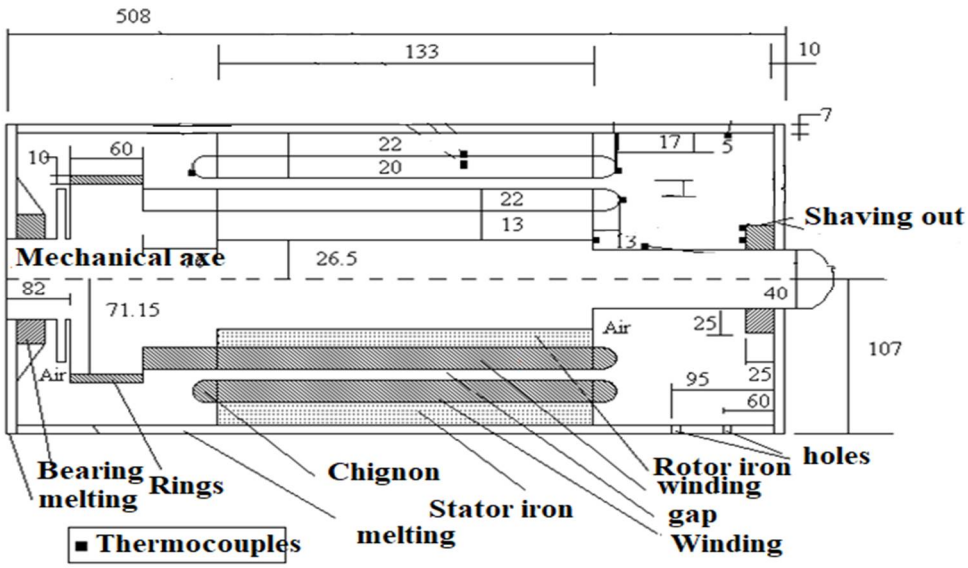

Figure 2: Axial view of the studied synchronous motor [20]

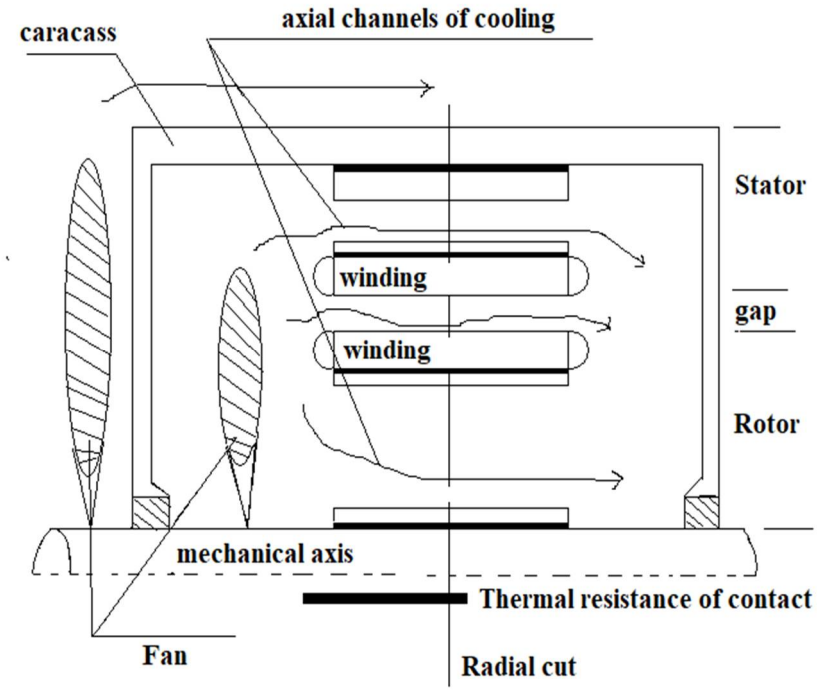

Figure 3: Axial half-cut of the studied engine

The absorbed power for a voltage between phase and neutral V_{ph}, for an intensity per phase I is a phase shift Φ between current and voltage is written by the following expression [21]

$$P_{ab} = 3V_{ph} I \cos\Phi \tag{1}$$

Joule losses in the stator are given by

$$P_{js} = 3R_{th} I^2 \tag{2}$$

Where R_{th} is the thermal resistance winding of a phase. The variation of this resistance as a function of the temperature is given by [22]

$$R_{th} = R_{th}(20°C)(1 + a\Delta T) \tag{3}$$

$$R_{th}(20°C) = R_0(20°C)(l / S) \tag{4}$$

where R_0 is the resistivity of the conductor at the reference temperature.

This formulation is valid when the current density is considered uniform in the conductor. In the case of higher frequencies, a skin effect increases the resistance [20]. The resolution of Maxwell's equations allows determining its expression as a function of the conductor's diameters and the skin thicknesses.

Note that the Joule losses in the rotor are due to the heating of the conductors within the rotor and are similar to those of the stator. In addition, the losses in the stator and rotor iron occur exclusively in the losses of the machines where the magnetic flux is valid.

The eddy current losses are due to the temporal variations of flux at the origin of electromotive forces in ferromagnetic materials and creating currents. These losses are usually expressed using the following approximated formula [23]:

$$P_f = \pi^2 . e^2 . B_m^2 . f^2 . V / 6R_0 \tag{5}$$

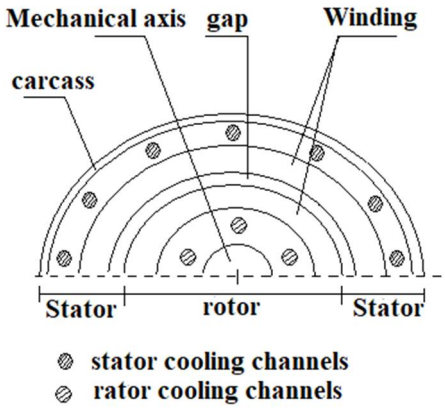

Figure 4: Radial half-cut of the studied engine

The mechanical losses concerning the friction losses of the trunnions, the brushes (collectors and rings), in the bearings that the losses by ventilation are often given by the following expressions:

- Friction losses of the brushes, given by:

$$P = F.\mathrm{b}.\mathrm{v} \tag{6}$$

- Friction losses in the bearings:

$$P = 2\pi NC_a \tag{7}$$

where C_a the friction torque of the tree.

The mechanical axis of the electric motor is shown in the form of a concentric cylinder, which is incorporated in the package of rotor plates and the stator plates concerning the outer carcass (see Figure 5). Then the thermal resistance R_{th} of a multilayer cylinder is given by the following expression [24]

$$R_{th} = \frac{1}{2\pi L}\sum_{i=1}^{n}\left[\frac{1}{\lambda}\ln\left(\frac{r_i}{r_{i-1}}\right)\right] \tag{8}$$

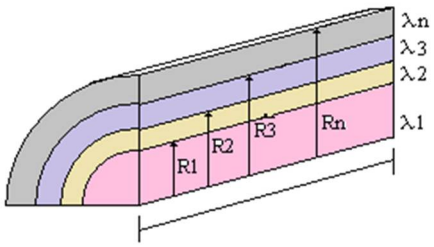

Figure 5: The thermal resistance of concentric cylinder

2.2 Thermal Model

The thermal model shows the relationships between the losses in the different parts of a rotating machine and the temperatures, considering the geometry and the heat exchange conditions. The different parts that make up our thermal model are the cast iron housing, the stator iron, the winding, the air gap, the rotor iron, and the mechanical axis.

To simplify the thermal model analysis, three hypotheses have been adopted to justify the modeling of the various constituent parts of the machine as a cylindrical elements:

1) The heat flows in the axial and radial directions are independent.
2) The average temperatures in both directions are independent.
3) No circumferential heat flows.

Thus, a cylindrical element, its dimensions, and its temperatures, given in figure 5, is used to model the different parts constituting the motor. For this simple geometry, the solution of differential transfer equations in both radial and axial directions allows obtaining an exact temperature distribution.

2.3 Fan choice

The most effective choice of the external fan, or blower, depends on many factors. The fans can be compared to each other based on the specific speed, an index to determine the most appropriate type of fan considering the flow rate, the pressure loss, and the speed of rotation. The specific speed is defined by[25]:

$$N_S = N\frac{\sqrt{q_V}}{\Delta p^{0,75}} \tag{9}$$

For each type of fan, the specific speed is within a certain range (table 3). Thus, there are only a limited number of combinations that give maximum efficiency. The necessary airflow is easily calculated by the following relation:

$$q_V = 0,83\frac{\varphi}{\Delta T_{air}} \tag{10}$$

Where φ is the power released in the equipment (W), and ΔT_{air} is the permissible increase of the air temperature (°C).

The third factor to be determined to calculate the rotation speeddepends on the available power supply, acoustic limits, service life, mass, and space requirement. In Table 1, we give the rotational speeds N most often used as a function of the available frequency. This simulation study is based on the experimental results carried out by Glises [26]on an asynchronous motor of 4 kW of power with an external fan. These experimental results are used as a data carrier for our simulation. For example, the separation of the Joule losses at the level of the various elements of the engine, the airflow, and the pressure losses, generated the thermophysical parameters of the engine elements.

Table 1: Speed range by fan motor type.

N_S	(1)	(2)	(3)	(4)	(5)	(6)	(7)	(8)
10^3								—
10^4		—	—	—	—	—	—	—
10^5	—		—	—	—	—	—	
10^6	—	—						

(1)- Propeller fan.
(2)- Axial tube fan.
(3)- Axial vane fan.
(4)- Squirrel cage fan: loose scroll.
(5)- Squirrel cage fan: tight scroll.
(6)- Centraxial fan.
(7)- Radial turbine fan.
(8)- High-pressure fan

3. Numerical Resolution

3.1 Nodal method

Traditionally, the temperature distribution within electrical machines is achieved using thermal networks [27]. This approach is still effective in determining the steady and transient states of temperature distribution. The model is developed from the geometric dimensions and the thermophysical properties of the materials constituting the machine. In addition, this method considers the machine assembly of homogeneous parts in construction and operation[28].

Instead, an equivalent thermal network type description is used, resulting in a simple representation. The losses then constitute the sources of currents, and the potential at the different nodes gives the temperature. The temperature is calculated only at the nodes of the network such that each node represents a subset of the machine in which the temperature is uniform. This method can deal with 1D, 2D, and 3D problems, and the equations can be nonlinear. The thermo-physical parameters are then functions of the temperature[29]. This method imposes the definition of a common parameter, the conductance, in the fluid and solid regions. The principle of such a method is simple:

1) The system is divided into several small but finite volumes.
2) It is assumed that each volume is isothermal at the temperature of its center.

3) The physical system is replaced by a network of fictitious, heat-conducting bars joining the centers (nodes) of the volumes.
4) Each bar is assigned a thermal conductance corresponding to that material between the nodes.

The heat flow transiting between two nodes is written in the form [30]:

$$\frac{dQ}{dt} = G.\left(T_j - T_i\right) \tag{11}$$

Where $G\left[W.K^{-1}\right]$ is the thermal conductance, and $T_i,\ T_j\left[K\right]$ is the isothermal temperatures of volumes i and j .

The different expressions of the flow and the conductance are given in the following table.

Table 2: Expressions of flows and conductance

Heat Transfer Mode	Flow expression	conductance Expression
Conductance	$\frac{\lambda S_{ij}}{L_{ij}}\left(T_j - T_i\right)$	$G_{ij}^{cond} = \frac{\lambda S_{ij}}{L_{ij}}$
Convection	$hS(T_S - T_i)$	$G_{is}^{conv} = hS$
Radiance	$\sigma S_i F_{ij}(T_j^4 - T_i^4)$, for black materials	$G_{ij}^{r} = \sigma S_i F_{ij}(T_j^2 + T_i^2)(T_i + T_j)$
Fluid flow	$mc(T_j - T_i)$	$G_{ij}^{f} = mc$

(1) S_{ij} volume exchange surface (*i*) and (*j*); L_{ij} Length between two nodes (*i*) and (*j*) (2) m mass flow [$kg.s^{-1}$]

In the case of a transient study, for a node (i) subjected to an internal source of heat and exchanging energy by conduction and radiation, the equation of heat flow is written by:

$$C_i \frac{dT_i}{dt} = \sum_{j=1}^{n} Gij^{cd}(T_j - T_i) + \sum_{j=1}^{n} Gij^{ray}(T_j - T_i) + \sum_{j=1}^{n} Gij^{cv}(T_j - T_i) + Q_i(t) \tag{12}$$

Writing this system to each node provides as many equations as there are nodes. The matrix formatting leads to:

$$\left[C_i\right].\left[\frac{dT_i}{dt}\right] = \left[G_{ij}\right].\left[T_i\right] + \left[Q_i\right] \tag{13}$$

Where $\left[C_i\right]$: the matrix of thermal capacities of the discretized volumes, $\left[G_{ij}\right]$: the matrix of the sum of the conductance's associating the volumes, $\left[Q_i\right]$: the heat source associated with the i^{th} node.

The different heat flows introduced for each node, according to the figure 6, are given by the following expressions:

$$\begin{cases} node(1): C_1 \dfrac{dT_1}{dt} = \dfrac{\lambda S_{12}}{L_{12}} T_1 + Q_1(t) \\ node(2): C_2 \dfrac{dT_2}{dt} = hST_2 + Q_2(t) \\ node(3): C_3 \dfrac{dT_3}{dt} = hST_3 \\ node(4): C_4 \dfrac{dT_4}{dt} = \dfrac{\lambda S_{45}}{L_{45}} T_4 + Q_4(t) \\ node(5): C_5 \dfrac{dT_5}{dt} = \dfrac{\lambda S_{56}}{L_{56}} T_5 + Q_5(t) \\ node(6): C_6 \dfrac{dT_6}{dt} = hST_6 + Q_1(t) \end{cases} \tag{14}$$

By taking $\frac{dT_i}{dt} = \frac{T_i^{i+1} - T_i^i}{\Delta t}$, the resolution of equations (14) is given as follows

$$\begin{cases} T_1^1 = T_1^0 + \frac{\Delta t}{C_1}\left[\frac{\lambda_1 S_{12}}{L_{12}} T_1^0 + Q_1\right] \\ T_2^1 = T_2^0 + \frac{\Delta t}{C2}\left[\left(hsT_2^0\right) + Q_2\right] \\ T_3^1 = T_3^0 + \frac{\Delta t}{C_3}\left[\left(hsT_3^0\right)\right] \\ T_4^1 = T_4^0 + \frac{\Delta t}{C_4}\left[\left(\frac{\lambda_4 S_{45}}{L_{45}}\right) T_4^0 + Q_4\right] \\ T_5^1 = T_5^0 + \frac{\Delta t}{C_5}\left[\left(\frac{\lambda_5 S_{56}}{L_{56}}\right) T_5^0 + Q_5\right] \\ T_6^1 = T_6^0 + \frac{\Delta t}{C_6}\left[\left(hsT_6^0\right)\right] \end{cases} \quad (15)$$

Knowing that: $T_6^0 = 24\,°C$ and S_{ij} are equal for all nodes.

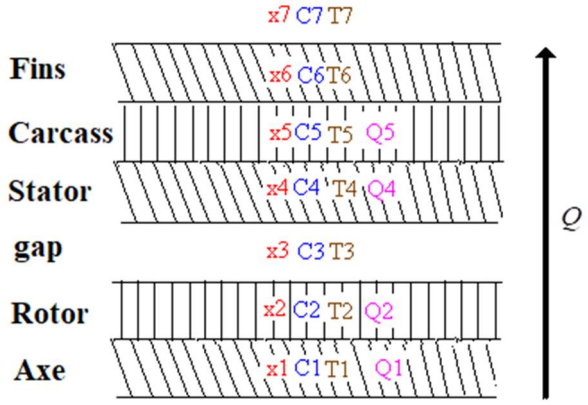

Figure 6: The different thermal source layers.

3.2 Computer Program

A computer program code written and compiled in the MATLAB environment, based on dimensions and thermo-physical data of engine components (shown in Table 3). The flow chart of the mentioned code is illustrated in Fig.7.

Table 3: Dimensional and thermo-physical data of the engine components [31]

Engine component	Radial distance $(10^{-3}m)$	Nodal distance $(10^{-3}m)$	Surface element (m^2)	Thermal conductivity (W/mK)	Joule losses (W)
Cast iron housing	7	4	0,1493	55,8	0
Stator iron	17	12	0,1395	62	0
Statoric winding	20	18,5	0,1158	0,5	241,10
Gap	0,35	10,17	0,0879	0,03	0
Rotor winding	22	11,17	0,0874	0,5	118,10
Rotor iron	13	17,5	0,0567	62	0
Mechanical axis	26,5	19,75	0,0386	45,8	0

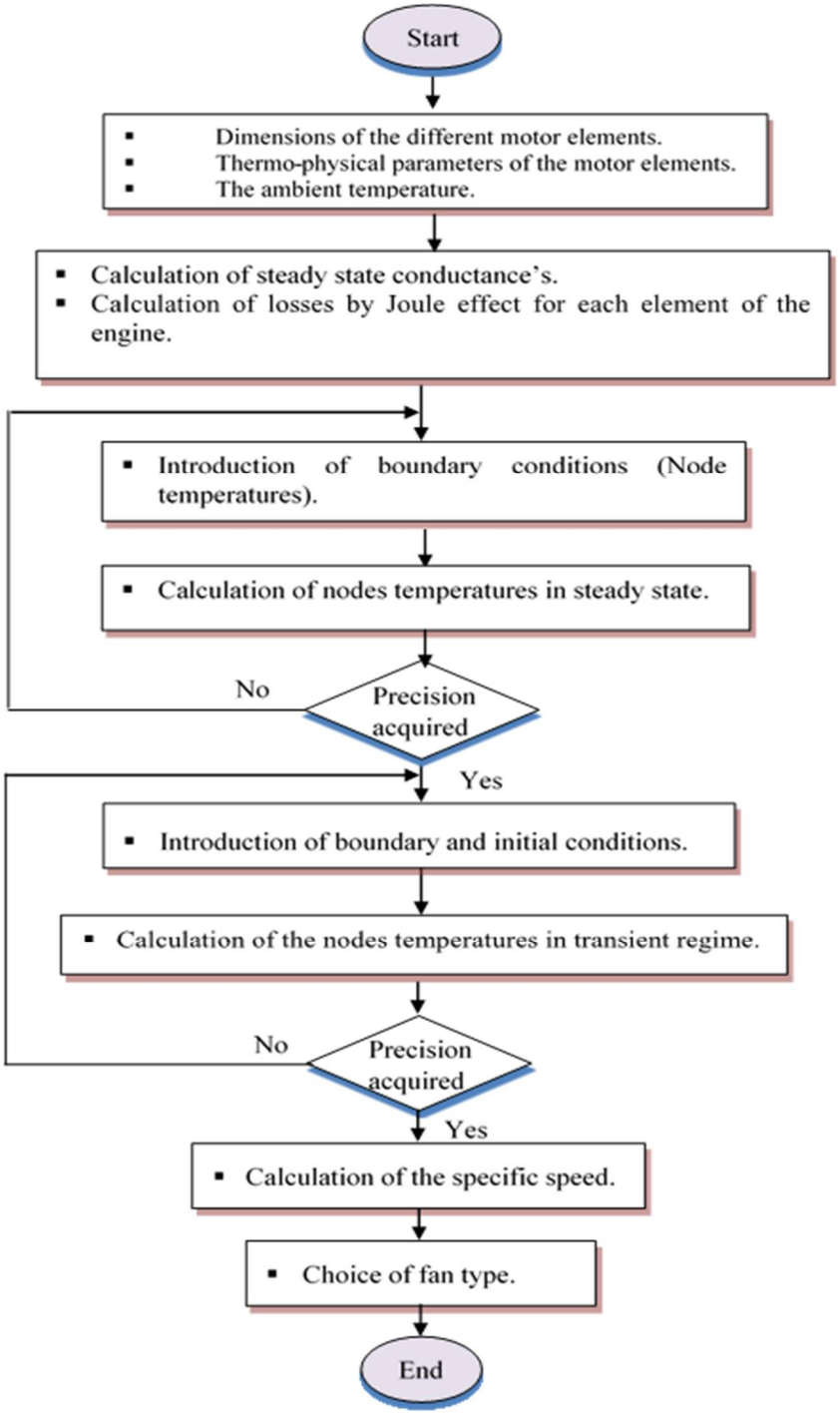

Figure 7: Flow-chart of the simulation method nodal.

3.3 Validation of Simulation

The presented results shown in table 4 are the simulated and the experimental heating temperature differences on an asynchronous electric motor in the reference laboratory [26]. For the same condition of operation at an ambient temperature $20°C$, it is noted that the relative error of the temperatures between the two results (numerical and experimental) within the motor elements (stator iron, rotor winding, stator winding, and the gap) is less than 8%. Therefore, there is a good agreement between the numerical and experimental results. Also, it is noted that the errors produced may be due to the reading of experimental measurements or the physical characteristics of the materials. Therefore, the mathematical model used to evaluate the thermal heating inside the asynchronous motor can represent the actual situation of normal operation. This means that the calculation program developed for this numerical approach can be used as a thermal performance optimization tool and allows measuring the most favorable operating conditions of asynchronous electric motors with low power. These permit selecting a good choice of engine cooling system.

Table 4: Comparison between the simulated and experimental heating temperatures.

Engine components	The experimental Temperature, ref [26]	The simulated Temperature (°C)	ΔT Temperature range	Error
Windings rotor	86 ,85	83,33	3,52	4,22%
Middle stator wind	60,53	65,64	5,11	7,78%
Bottom stator wind	55,87	52,98	2,89	5,17%
Middle stator iron	52,31	48,32	3,99	7,62%

4. Results And Discussions

4.1 Permanent Temperature Distribution ($T_{amb} = 20°C$)

The temperature distribution within the motor is an increasing function with the radial distance. From Figure 8, it can be seen that the temperature at the surface of the cast iron housing is equal to the ambient temperature. As the radial distance increases, it is noted that the temperature increases linearly by $20°C$ crankcase up to almost $130°C$ at the mechanical axis. The rapid temperature growth at the stator and rotor winding is the Joule effect losses in these two motor elements. The conductance matrix and the permanent temperature distribution within the engine are found as follows:

$$T_p = [20\ \ 20\ \ 97,052\ \ 97,052\ \ 27,257\ \ 27,257\ \ 27,257]$$

$$G = 10^{+3}[2,0970\ \ 0,7207\ \ 0,0031\ \ 0,0003\ \ 0,0039\ \ 0,2009\ \ 0,0894]$$

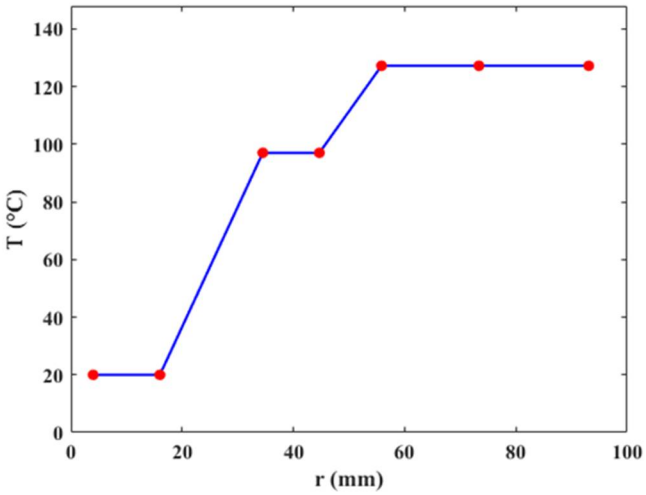

Figure 8: The permanent temperature distribution within the asynchronous motor for an ambient temperature of $T_{amb} = 20°C$

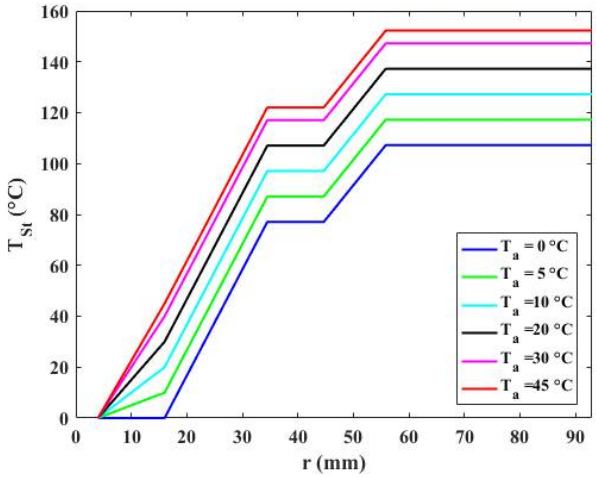

Figure 9: Effect of ambient temperature on permanent temperature field within the asynchronous motor

4.2 Effect of Ambient Temperature on Permanent Temperature Distribution

Figure 8 shows the effect of the ambient temperature on the permanent temperature field within the engine. Clearly, this figure shows that the permanent temperature increases mostly linearly with increasing radial distance (starting from the cast iron housing, stator iron, stator winding, air gap, rotor winding, and rotor iron towards the mechanical axis). The increase in temperature within the engine is mainly due to the Joule heat losses at the stator and rotor winding. The ambient temperature increase is clear on electric motor heating while operation, i.e. the permanent temperature for each engine element increases proportionally with increased ambient temperature.

4.3 Transient Temperature Distribution $\left(T_{amb} = 20°C\right)$

Figures 10 and 11 show the transient temperature evolution within the externally cooled asynchronous motor. In particular, Figure 10 illustrates this evolution, shown as a contour plot indicating isothermal lines in the various engine elements. In contrast, Figure 11 shows the same mentioned evolution as the surface plot, which allows determining the engine hotspots (i.e., hottest elements) as a function of time.

It is worth noting that the engine heats up over time. Except for the first seconds when the different motor elements are almost at room temperature, the temperature increases in the elements from the mechanical axis, the rotor iron, the rotor winding, etc., to the cast iron housing, or the is close to the ambient temperature. The reason behind the inner elements' heating problem is that the Joule effects losses are mainly generated in the stator or rotor windings.

4.4 Effect of Ambient Temperature on Transient Temperature Distribution

The effects of the ambient temperature on the transient temperature distribution within the asynchronous electric motor are shown in figure 12 according to the considered ambient temperature values. The most significant observation is that the increase of the ambient environment temperature where the motor operates enables the appearance of the hot zones, especially at the engine elements level, which manifests thermal losses by the Joule effect, namely, winding stator and rotor winding.

For example, if we compare the thermal behavior of the engine at an ambient temperature $5°C$ with that demonstrated at $45°C$ a time interval of 120 seconds. We can discern that the motor $5°C$ will begin to heat by the Joule effect at its internal elements level as soon as the first 70th-second pass, while the hot zones appear within the engine for an ambient temperature of $45°C$ the first 3 seconds. This interprets the easy appearance of the hot zones within the engine under the effect of the ambient temperature.

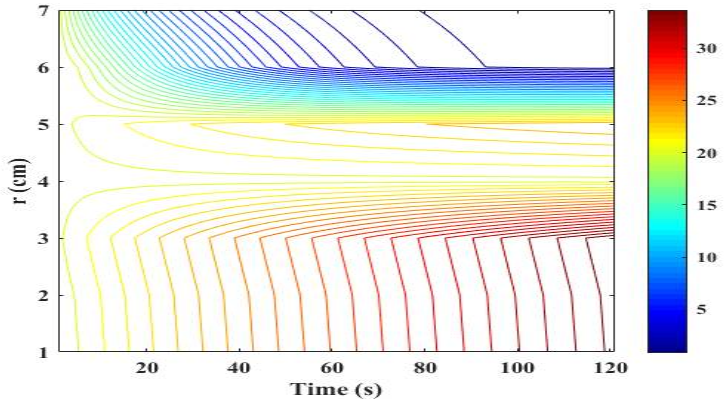

Figure 10: Transient temperature evolution (contour representation) within the asynchronous motor for an ambient temperature $\left(T_{amb} = 20°C\right)$

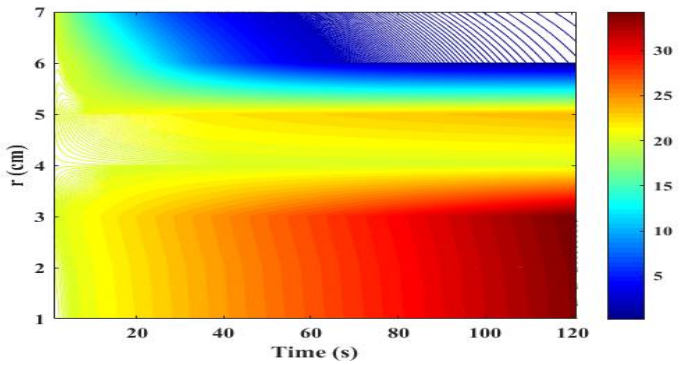

Figure 11: Transient temperature temporal evolution (surface representation) within the asynchronous motor for an ambient temperature $\left(T_{amb} = 20°C\right)$

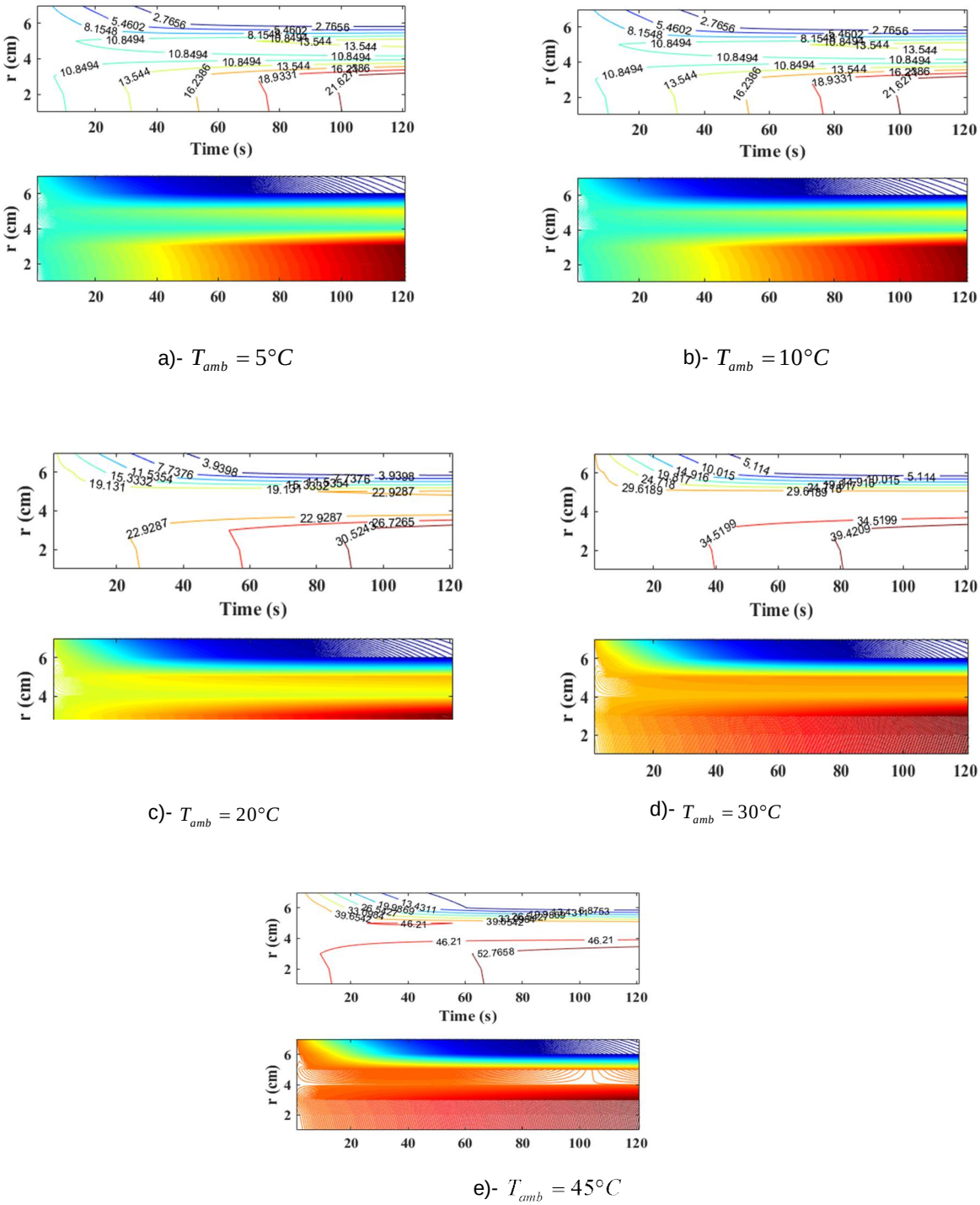

Figure 12: Transient temperature time-evolution (contour and surface plots) within the asynchronous motor for different ambient temperatures

The second observation concerning the ambient temperature effect is that the engine's heating following the latter's effect is predominant in depth. This is because it covers almost all the elements in the radial direction as the temperature of the surrounding environment increases.

The effect of the operating time on the distribution of the transient temperature within the asynchronous electric motor is shown in figure 13, corresponding to the operation time taken by the asynchronous electric motor.

We observe that the increase of this time interval is accompanied by a very considerable temperature increase within the various engine elements and, more specifically, the appearance of the hot zones at the engine elements level, which manifest thermal losses by the Joule effect, namely, the stator and rotor windings.

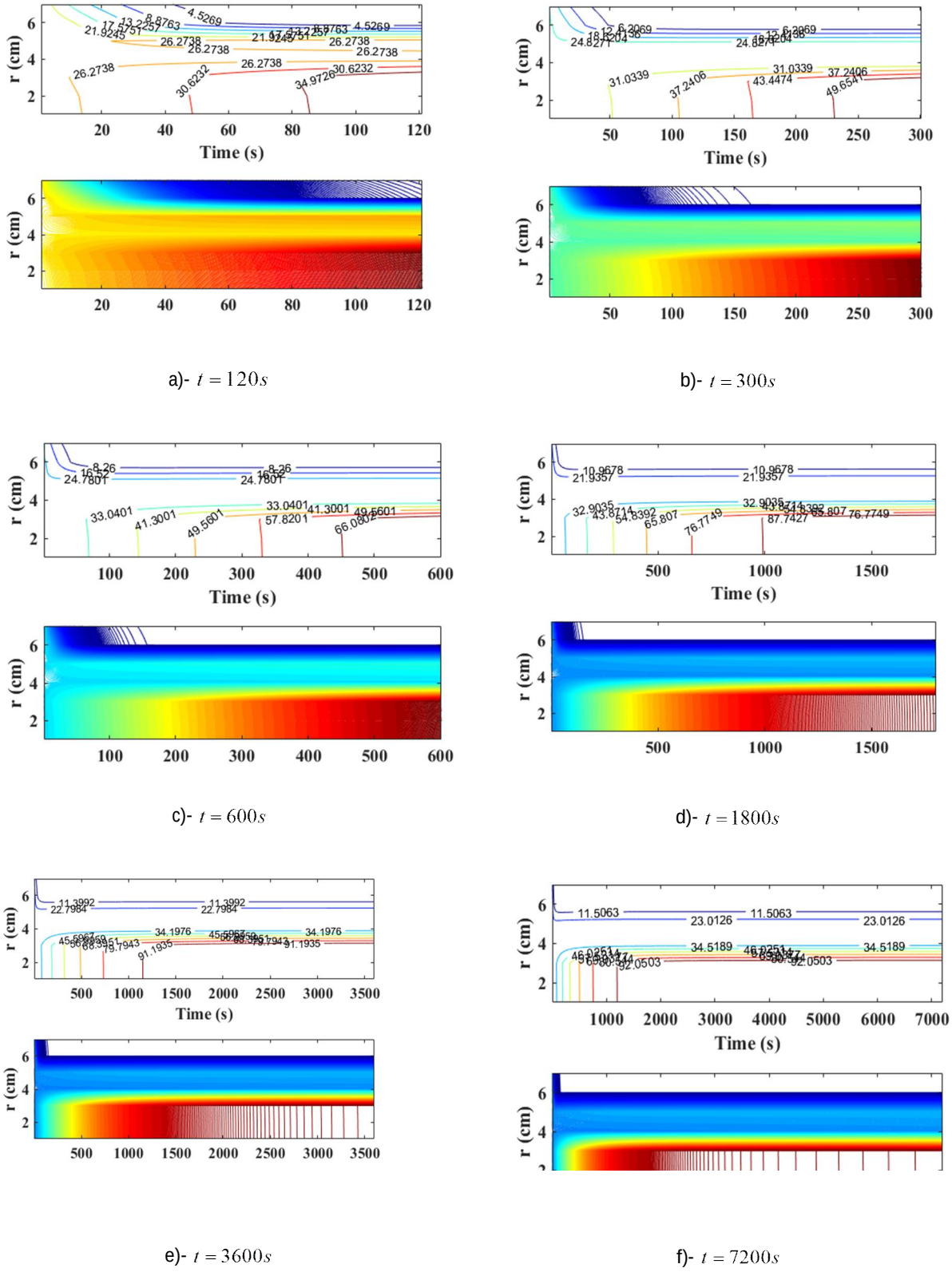

Figure 13: Transient temperature histories within the engine elements for different time intervals $(T_{amb} = 25°C)$

The comparison between the engine thermal behavior at a time interval of 120 seconds and that over 1800 seconds shows that the maximum inner temperature reached in the first period is in the order of $20°C$. In contrast, the hot zones that appear within the engine for the second period have temperature values $80°C$ for an ambient temperature of $20°C$. This elucidates the possible appearance of hot zones within the engine during the asynchronous electric motor's operating time.

5. Conclusion

In this study, we have dealt with applying the nodal numerical method to determine the heating behavior of an asynchronous electric motor. The study aimed to predict the permanent and transient temperature fields within each element of this machine, namely the cast iron housing, stator iron, stator winding, air gap, rotor winding, rotor iron, and the mechanical axis. The approach of this simulation is based on the dimensional and thermo-physical data of an electric engine with low power of 4 kW. This numerical approach shows that the engine heating is mainly owed to the thermal losses caused by the Joule effect at various motor elements, which is explained by very hotspots at the stator and rotor windings. Furthermore, by analyzing the ambient temperature effect on the heating engine, we have concluded that the increase of this latter causes the appearance of the very hot zones leading to the heating engine's phenomenon.

The procedure calculates the motor's specific speed according to its rotation speed, the volumetric air flow rate, and the fan-load losses for the fan's choice. Using the table giving the appropriate external cooling fan types according to the required specific speed allows us to choose the engine cooling system adequately.

Nomenclature

P_{ab}	Absorbed power (W)
C	Thermal capacity
P_{js}	Joule losses in the stator (J)
R_{th}	Thermal resistance winding (K/W)
R_0	The resistivity of the conductor at the reference temperature
G	Thermal conductance
Q	Heat flux (W)
S	Surface (m^2)
L_{ij}	Length between two nodes (i and j)
λ	Thermal conductivity (W/mK)
h	Coefficient of thermal convection (W/m^2K)
N_S	The specific speed of the fan (tr/min)
φ	The power released in the equipment
ΔT_{air}	Permissible increase of the air temperature
T	Temperature (K)
T_{amb}	Ambient temperature (K)
T_P	Permanent temperature (K)
r	Radial distance (m)
t	Time (s)

Author contribution

All authors contributed equally to this work.

Funding

This research received no external funding

Data availability statement

The data that support the findings of this study are available on request from the corresponding author.

Conflicts of interest

Authors declare that their present work has no conflict of interest with other published works.

References

[1] T. I. Kang, C. O. Ahn, I. S. Seo, and S. H. Lee, Numerical analysis for prediction of flow rate of the motor cooling fan, J. Mech. Sci. Technol., 22 (2008) 1870-1875.

[2] S. Moon and S. Lee, High-Reliable Temperature Prediction Considering Stray Load Loss for Large Induction Machine, IEEE Trans. Magn., 55 (2019) 1-5. https://doi.org/10.1109/TMAG.2019.2901862

[3] Y. Gai, M. Kimiabeigi, Y. C. Chong, J. D. Widmer, X. Deng, M. Popescu, *et al.*, Cooling of Automotive Traction Motors: Schemes, Examples, and Computation Methods, IEEE Trans. Ind. Electron., 66 (2018) 1681-1692 . https://doi.org/10.1109/TIE.2018.2835397

[4] A. Boglietti, M. Cossale, M. Popescu, and D. A. Staton, Electrical Machines Thermal Model: Advanced Calibration Techniques, IEEE Trans. Ind. Appl., 55(2019) 2620-2628, https://doi.org/10.1109/TIA.2019.2897264

[5] M. Grabowski, K. Urbaniec, J. Wernik, and K. J. Wołosz, Numerical simulation and experimental verification of heat transfer from a finned housing of an electric motor, Energy Convers. Manage., 125 (2016) 91-96, https://doi.org/10.1016/j.enconman.2016.05.038

[6] V. Satiraman and R. Saxena, Steady state thermal analysis of electrical machines by EF method, J. Jnsr. Eng. Elect. Eng. Div., 64 (1984) 201-206.

[7] M. Popescu, D. Staton, A. Boglietti, A. Cavagnino, D. Hawkins, and J. Goss, Modern heat extraction systems for electrical machines-A review, in 2015 IEEE Workshop on Electrical Machines Design, Control and Diagnosis (WEMDCD), 2015, 289-296. http://dx.doi.org/10.1109/WEMDCD.2015.7194542

[8] D. Staton, A. Boglietti, and A. Cavagnino, Solving the more difficult aspects of electric motor thermal analysis, in IEEE Int. Electric Mach. . Driv. Conf., IEMDC'03., 747-755,2003 http://dx.doi.org/10.1109/TEC.2005.847979

[9] V. Sreenivasan and D. Sengupta, Thermal Design of Totally Enclosed Fan Cooled Induction-Motors, IEEE Trans. Power Appar. Syst., (1977) 1072-1072.

[10] P. Dokopoulos and J. Xypteras, Analysis of transient temperature distribution in a rotating machine, Int. Conf. Electr. Mach. Syst., 5-9 , 1982.

[11] D. Staton, D. Hawkins, and M. Popescu, Thermal Behaviour of Electrical Motors–An Analytical Approach, in INDUCTICA Techn. Conf. Program, CWIEME, Berlin, 5-7 , 2009.

[12] Z. Tan, X.-g. Song, B. Ji, Z. Liu, J.-e. Ma, and W.-p. Cao, 3D thermal analysis of a permanent magnet motor with cooling fans, in China's High-Speed Rail Technology, J. Zhejiang Univ. Sci.,Springer, 577-587 , 2018.

[13] K. Sim, Y.-B. Lee, S.-M. Jang, and T. H. Kim, Thermal analysis of high-speed permanent magnet motor with cooling flows supported on gas foil bearings: part I-coupled thermal and loss modeling, J. Mech. Sci. Technol., 29 (2015) 5469-5476.

[14] B. Melka, J. Smolka, J. Hetmanczyk, and P. Lasek, Numerical and experimental analysis of heat dissipation intensification from electric motor,Energy, 2019. https://doi.org/10.1016/j.energy.2019.06.023

[15] G. Kramer, G. Szepesi, and Z. Siménfalvi, Novel hot air engine and its mathematical model–experimental measurements and numerical analysis, Pollack Periodica, 14 (2019) 47-58. https://doi.org/10.1556/606.2019.14.1.5

[16] J. Nonneman, B. Van der Sijpe, I. T'Jollyn, S. Vanhee, J. Druant, and M. De Paepe, Evaluation of High Performance Rotor Cooling Techniques for Permanent Magnet Electric Motors, *2021* IEEE Int. Electric. Mach. Driv. Conf., 1-7, 2021. https://doi.org/10.1109/IEMDC47953.2021.9449603

[17] Y. Sun, S. Zhang, G. Chen, Y. Tang, and F. Liang, Experimental and numerical investigation on a novel heat pipe based cooling strategy for permanent magnet synchronous motors, Appl. Therm. Eng., 170 (2020) 114970. https://doi.org/10.1016/j.applthermaleng.2020.114970

[18] E. Gundabattini, R. Kuppan, D. G. Solomon, A. Kalam, D. Kothari, and R. A. Bakar, A review on methods of finding losses and cooling methods to increase efficiency of electric machines, Ain Shams Eng. J., 12 (2021) 497-505. https://doi.org/10.1016/j.asej.2020.08.014

[19] Q. Chen and X. Yang, Calculation analysis of thermal loss and temperature field of in-wheel motor in micro-electric vehicle, J. Mech. Sci. Technol., 28 (2014) 3189-3195.

[20] R. Glises, G. Hostache, and J. Kauffmann, Simulation du comportement thermique en régime permanent d'un moteur asynchrone à refroidissement extérieur. Etude par éléments finis, J. Phys. III, 4 (1994) 1723-1735.

[21] D. Roye and R. Perret, Définitions des règles de modélisation thermique des machines électriques tournantes, Revue de physique appliquée, 20 (1985) 191-202.

[22] N. Burais, Etude et modelisation des Pertes dans les circuits magnetiques en Regime Non Sinusoidal a Frequence Industrielle Elevee,1981.

[23] J. Chatelain, Machines électriques vol. 10: Ppur Presses polytechniques, 1989.

[24] F. P. Incropera, A. S. Lavine, T. L. Bergman, and D. P. DeWitt, Fundamentals of heat and mass transfer: Wiley, 2007.

[25] H. G. Johnson, Electric fan motor, ed: Google Patents, 1997.

[26] R. Glises, A. Miraoui, and J. Kauffmann, Thermal modelling for an induction motor, J. Phys. III, 3 (1993) 1849-1859,

[27] M. Bouheraoua, Contribution à la modélisation thermique d'un moteur asynchrone à cage, Université Mouloud Mammeri, 2008.

[28] R. Khaldi, Etude expérimentale du comportement thermique du moteur asynchrone alimenté par convertisseur, 1996.

[29] Bouheraoua M. , Contribution à la modélisation thermique d'un moteur asynchrone à cage, Université Mouloud Mammeri, 2008.

[30] Khaldi R. Etude expérimentale du comportement thermique du moteur asynchrone alimenté par convertisseur, 1996.

[31] H. Cortès and J. Blot, Transferts thermiques application à l'habitat: étude par la méthode nodale: Ellipses/ed. marketing SA, 1999.

[32] Fraudet H. , Cours d'électricité tome 1.

[33] R. Glises de la Rivière, Etude théorique et expérimentale des flux thermiques dans un moteur asynchrone à refroidissement extérieur, Besançon, 1994.